JOURNAL OF CATALYSIS 155, 290–302 (1995)

NO Adsorption, Decomposition, and Reduction by Methane over Rare Earth Oxides

Xiankuan Zhang, Arden B. Walters, and M. Albert Vannice[1]

Department of Chemical Engineering, The Pennsylvania State University, University Park, Pennsylvania 16802-4400

Received January 23, 1995; revised April 25, 1995

Adsorption and decomposition of NO and its reduction by methane have been conducted over La_2O_3, CeO_2, Nd_2O_3, Sm_2O_3, Tm_2O_3, and Lu_2O_3 as well as Sr-promoted LaO_3 and Sm_2O_3. NO was irreversibly adsorbed on all these rare earth oxide (REO) catalysts at 300 K, and the uptakes per unit surface area were $2.5 \pm 1.0 \times 10^{18}$ molecules/m^2 except on CeO_2, which had a lower uptake. On La_2O_3 and Sm_2O_3, no significant CH_4 chemisorption occurred at 300 or 573 K, while oxygen did not chemisorb at 300 K and only small irreversible uptakes were detected at 573 K. Both NO decomposition in He and NO reduction by CH_4 were conducted in a quartz microreactor between 773 and 973 K; all the REO catalysts were active for either reaction in both the absence and presence of O_2. Activities increased continuously with increasing temperature and no deactivation or bendover was observed except for Sm_2O_3, over which complete combustion of CH_4 occurred at high temperature in the presence of O_2. The specific activities for NO reduction to N_2 by CH_4 were higher than those for NO decomposition, and CH_4 reduction of NO gave selectivities to N_2 that were near 100% for all the catalysts except Sr/La_2O_3, Sm_2O_3, and Sr/Sm_2O_3, over which 5–20% N_2O was formed. Except for CeO_2, the presence of O_2 promoted the rate of NO conversion to N_2. Overall, Sr/La_2O_3 had the highest specific activity for NO reduction by CH_4 in either the absence or presence of O_2, with respective values of 4.6×10^{-3} and 13×10^{-3} μmole $N_2/s \cdot m^2$ at 773 K. Turnover frequencies under these two sets of conditions, based on NO adsorption, were 0.78×10^{-3} and 2.3×10^{-3} s^{-1}, respectively. Activation energies fell between 22 and 32 kcal/mole for all the REOs. The highest specific activities for NO decomposition to N_2 occurred on Sm_2O_3 and Nd_2O_3 and were 1.6×10^{-3} and 1.1×10^{-3} μmol $N_2/s \cdot m^2$ at 773 K; these correspond to TOFs of 3.6×10^{-4} and 4.3×10^{-4} s^{-1}, respectively. Activation energies for NO decomposition ranged from 21 to 29 kcal/mole. The best REO catalysts correlated with those best for the oxidative coupling of methane. On a TOF basis, the best REO catalysts were comparable to Co/ZSM-5.

[1] To whom correspondence should be addressed.

INTRODUCTION

The reduction of NO_x (NO and NO_2) to N_2 in the presence of dioxygen is a challenging and important reaction because of its application to both stationary and mobile sources, and it has attracted much attention in recent years (1, 2). The three-way automotive catalysts, based on the use of combinations of noble metals, have been highly successful in controlling exhaust emissions from conventional gasoline engines operating close to stoichiometric conditions. However, the exhaust from lean-burn gasoline engines and from diesel engines contains over 5% oxygen and, under these net oxidizing conditions, the three-way catalysts cannot convert NO_x to sufficiently low levels although CO and hydrocarbon emissions are still controlled (1). In addition to this situation, the use of ammonia as a reducing agent to remove NO_x emitted from stationary sources under net oxidizing conditions creates problems of its own, such as NH_3 transportation and storage hazards, equipment corrosion, and NH_3 slip. A hydrocarbon reductant—especially CH_4, which is the major component in natural gas—could provide a markedly improved emission control system.

Metal ion-exchanged zeolite catalysts have now been shown to be active for either the direct decomposition of NO (3–5) or the selective reduction of NO by hydrocarbons, including methane (6–13). It was discovered that the presence of excess O_2 enhanced activities for NO reduction over many of these zeolite-based catalysts; however, a volcano-like activity dependence on temperature, which decreases NO reduction at higher temperatures and limits the suitability of these catalysts in some applications, was typically observed. The stability of these zeolites in the presence of water vapor also presents a problem; therefore, there is a need for alternative nonzeolite catalyst systems. Two nonzeolite catalyst systems (Li/MgO and La_2O_3) for NO reduction by CH_4 have been prepared and characterized and then used to test a new concept—the activation of CH_4 on oxidative coupling catalysts to effectively reduce NO_x (14, 15). Li/MgO and La_2O_3 were initially chosen

0021-9517/95 $12.00

TABLE 1

BET Surface Areas (m^2/g) of Rare Earth Oxides

Catalyst	Fresh	Used
La_2O_3	3.7	3.5
Sr/La_2O_3	1.9	1.7
CeO_2	2.3	2.5
Nd_2O_3	3.5	3.4
Sm_2O_3	7.5	7.3
Sr/Sm_2O_3	6.9	6.8
Tm_2O_3	0.96	0.94
Lu_2O_3	2.3	2.4
Li/MgO	3.7	3.5
Co/ZSM-5[a]	193	—

[a] Supplied by Air Products.

because they are two of the best catalysts for methane oxidative coupling (MOC). Both catalysts were found to be active for NO reduction by CH_4 but, unlike the zeolites, the activities exhibited no bendover and continuously increased with reaction temperature. In this paper a study is presented of NO adsorption, decomposition, and reduction by CH_4 in both the absence and presence of O_2 over a family of rare earth oxide (REO) catalysts. For comparison, corresponding results obtained with Li/MgO and Co/ZSM-5 are also included and discussed.

EXPERIMENTAL

The following pure REO samples were prepared by calcining the corresponding commercial oxides at 1023 K for 10 h under flowing dry air (~50 cm^3 (STP)/min): La_2O_3 (Rhone-Poulenc, 99.99%), CeO_2 (Rhone-Poulenc, 99.9%), Nd_2O_3 (Sigma, 99.9%), Sm_2O_3 (Sigma, 99.9%), Tm_2O_3 (Rhone-Poulenc, 99.99%), and Lu_2O_3 (Rhone-Poulenc, 99.99%). The doped samples of 4 wt% Sr/La_2O_3 and 4 wt% Sr/Sm_2O_3 were prepared as follows (16): appropriate amounts of $Sr(NO_3)_2$ (Aldrich, 99.995%) and La_2O_3 or Sm_2O_3 were added to distilled and deionized water, and the resulting slurry was then stirred and heated until only a thick paste remained. To ensure that a completely homogeneous catalyst was obtained, a fresh portion of water was added to the paste; this procedure was repeated two more times. The resulting paste was dried in air at 400 K overnight, ground into powder, and then calcined at 1023 K for 10 h under flowing dry air (~50 cm^3 (STP)/min). The 4% Co/ZSM-5 sample was obtained from Li and Armor (5, 6). The BET surface area measurements were carried out with a Quantasorb system, and the values for both the fresh and used samples are presented in Table 1.

Chemisorption of NO, CH_4, and O_2 was determined volumetrically in a vacuum system with a base pressure of $\leq 1 \times 10^{-6}$ Torr (1 Torr = 133.3 Pa). Adsorption isotherms were obtained using a new Mensor DPGII Model 15000 pressure transducer with 0.01% F.S. accuracy. Prior to the volumetric measurements for each probe molecule, the sample was subjected to, unless otherwise specified, a standard pretreatment consisting of calcination at 973 K for 30 min under flowing 10% O_2/90% He to remove residual carbon-containing surface species followed by either evacuation at 973 K for 30 min before cooling to 300 K (referred to as an evacuated sample), or cooling to 300 K in 10% O_2/90% He (referred to as an oxidized sample). The sample was continuously evacuated until the base pressure was achieved (approximately 30 min), then the adsorbate was introduced. The same procedures apply to adsorption at 573 K, in which case the sample was cooled to and maintained at 573 K instead of 300 K.

All the volumetric measurements were conducted at pressures between 40 and 160 Torr. After evacuation to the base pressure, which again took about 30 min, a second isotherm was measured to determine reversible adsorption. In general, the first pressure measurement of the isotherm was taken after an equilibration period of 30 min for CH_4 and O_2 and 60 min for NO, while subsequent pressure measurements usually stabilized in less than 20 and 30 min, respectively. The He and O_2 (MG Industries, 99.999%) were purified by passage through drying tubes containing a 5A molecular sieve, while NO (MG Industries, 99.0+%) was used without further purification.

All activity measurements and kinetic studies were made at atmospheric pressure under steady-state conditions in a quartz microreactor system which has been described in detail in a previous paper (14). NO decomposition runs were conducted with 2.0% NO in He while, unless otherwise specified, a typical gas mixture of 2.0% NO, 0.51% CH_4 in He, i.e., a stoichiometric ratio of $NO:CH_4 = 4:1$ according to the reaction $4NO + CH_4 \rightarrow 2N_2 + CO_2 + 2H_2O$, was passed through the reactor containing 0.1 g catalyst (0.2 g for La_2O_3). All gases used, i.e., 4.04% NO in He, 1.01% CH_4 in He, 9.8% O_2 in He, and pure He were UHP grade from MG Industries except for the NO mixed in He, which was 99.0+% with major mixture impurities of N_2 (~600 ppm), N_2O (~100 ppm), and traces of CO_2.

It was found that all the REO catalysts, either fresh or after use with CH_4, always contained some residual surface carbon species and this residual carbon was active for NO reduction (15). Before any data were taken, the samples were therefore pretreated at 973 K in a 9.8% O_2/He mixture at a flow rate of 20 cm^3 (STP)/min until no CO_2 was detected, thus eliminating the possibility of NO reduction by residual carbon contained on the catalyst. However, residual carbon inevitably developed on the catalyst surface under reaction conditions in the presence of CH_4 because some CO_2 was detected when the used sample was pretreated in 9.8% O_2 as above. This residual

carbon may actually play an important role in NO reduction (10).

During the Arrhenius runs, a period of 30 min on stream was allowed at each temperature before any gas sample was taken. An ascending-temperature sequence from 773 to 973 K was usually followed by a descending-temperature sequence in order to check for any deactivation during these measurements. The conversions were generally kept below 20% to approach differential reactor operation. The kinetic studies in the presence of gas-phase oxygen were carried out by adding a mixture of 9.8% O_2 in He to the feed containing NO and CH_4.

The reactor effluent was analyzed with a gas chromatograph (Perkin–Elmer Sigma-2B) equipped with a Carboxen^{1000} column (Supelco) and a P-E Nelson 1020S integrator (14). In the absence of gaseous O_2, good nitrogen and carbon mass balances (±2.5%) were obtained. Because of the gas-phase reaction of NO and O_2 and possible formation of other nitrogen oxides such as N_2O and NO_2, even in the absence of gaseous oxygen, NO consumption is not an accurate measure of the degree of NO reduction to N_2. Therefore, rates or specific activities for NO reduction to N_2 are expressed as the number of N_2 molecules produced per second per gram (μmol/s·g) or square meter (μmol/s·m^2) of catalyst. Background impurity levels of N_2 and N_2O in the cylinder gas (4.04% NO/He) were subtracted from the total amounts of N_2 and N_2O detected. The turnover frequencies (TOFs) for NO decomposition and NO reduction by CH_4 were obtained by dividing the rate (μmol/s·g) by the irreversible NO uptake (μmol/g) at 300 K. Gas hourly space velocities were based upon the apparent bed densities in the reaction, which varied from 0.9 to 2.7 g/cm^3; consequently, since feed gas flow rates were constant, GHSV varied from 17,400 to 63,800 h^{-1}. In the presence of oxygen, methane can react not only with nitric oxide, but also directly with O_2 via combustion. These two reactions,

$$CH_4 + 4NO \rightarrow 2N_2 + CO_2 + 2H_2O \quad [1]$$

and

$$CH_4 + 2O_2 \rightarrow CO_2 + 2H_2O, \quad [2]$$

are competitive. The selectivity, S, for methane reduction of NO to N_2 is defined here as methane consumed in the reduction reaction divided by total methane converted; i.e.,

$$S = \frac{\text{Rate (1)}}{\text{Rate (1)} + \text{Rate (2)}}. \quad [3]$$

RESULTS

Chemisorption

Table 2 lists the irreversible uptakes of NO at 300 K on the evacuated rare earth oxides as well as Li/MgO and Co/ZSM-5. As an example, Fig. 1 shows the adsorption isotherms for NO on La_2O_3. The first isotherm represents both irreversible and reversible adsorption while the second one measures only reversible adsorption, thus the difference gives the irreversible uptake of 13.1 μmole/g, which has an independence of pressure that indicates saturation coverage of these sites. Considering the low surface areas of the REO catalysts, the uptakes are relatively high and approximately 5–20% of the surface appears to be covered. Sr/La_2O_3 and Tm_2O_3 had the highest irreversible NO uptakes per m^2, followed by Lu_2O_3, while CeO_2 had the lowest. Doping with Sr noticeably enhanced the adsorption site density on La_2O_3, while the site density on Sr/Sm_2O_3 decreased. The irreversible NO uptake per gram on 4% Co/ZSM-5 was 1–2 orders of magnitude higher than those on the REO catalysts, as essentially 1 NO molecule ad-

TABLE 2

NO Chemisorption on Evacuated Rare Earth Oxides at 300 K

Catalyst	Irreversible NO uptake (μmol/g)	Irreversible NO uptake (molecule/m^2 × 10^{-18})
La_2O_3	13.1	2.3
Sr/La_2O_3	10.0	3.5
CeO_2	4.3	1.0
Nd_2O_3	9.0	1.6
Sm_2O_3	32.8	2.7
Sr/Sm_2O_3	20.7	1.8
Tm_2O_3	5.5	3.5
Lu_2O_3	12.2	3.1
Li/MgO	2.6	0.45
4% Co/ZSM-5	560	1.7[a]

[a] Based on BET surface area.

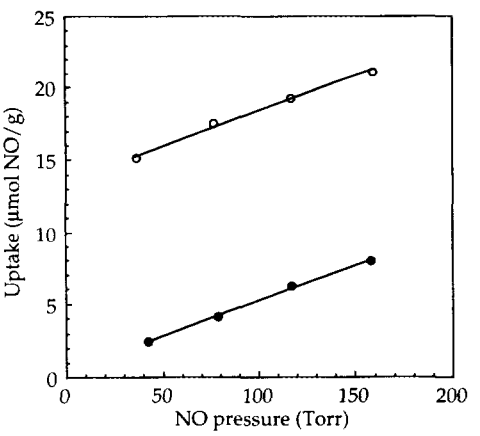

FIG. 1. Adsorption isotherms for NO on La_2O_3 at 300 K: (○) first isotherm and (●) second isotherm.

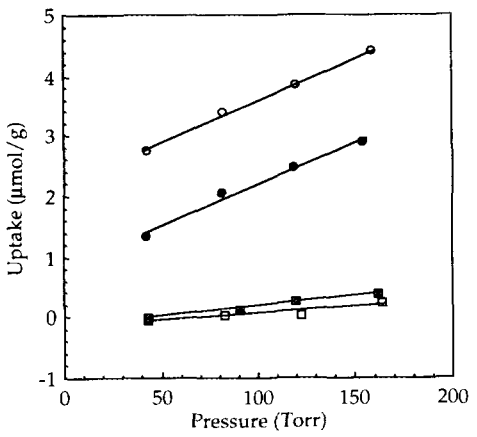

FIG. 2. Adsorption isotherms on La_2O_3 at 573 K: O_2, (○) first isotherm and (●) second isotherm; CH_4, (□) first isotherm and (■) second isotherm.

sorbed per Co exchange site. The Li/MgO sample had both the lowest NO uptake and the lowest site density.

The effect of different pretreatments on NO chemisorption on La_2O_3 was also examined. The irreversible NO uptake on oxidized La_2O_3 was only 6.0 μmol/g, which was about half that obtained on the evacuated sample. The adsorption of O_2 on reduced La_2O_3 at 300 K was completely reversible and did not affect the following irreversible NO uptake as the uptake remained the same (13.0 μmol/g). NO adsorption at the higher temperature of 573 K on evacuated La_2O_3 produced a lower irreversible uptake of 11.0 μmole/g. Oxygen and methane chemisorption was also conducted on La_2O_3 and Sm_2O_3 at 300 and 573 K. No irreversible CH_4 uptake occurred at either temperature on these two samples after any pretreatment employed in this work, as indicated by Fig. 2, and the two isotherms were essentially the same within experimental error. Even the reversible uptakes of CH_4 were very small. These results show that little or no CH_4 adsorption occurs at these low temperatures under our conditions. Similar results were observed for O_2 chemisorption at 300 K; however, significant irreversible O_2 adsorption occurred at 573 K on evacuated samples of La_2O_3 and Sm_2O_3, i.e., respective uptakes were 1.4 and 1.0 μmol/g. Figure 2 also shows the adsorption isotherms for O_2 on La_2O_3 at 573 K.

NO Decomposition

Small amounts of residual carbon on the REOs were present initially, presumably in the form of carbonates because of the propensity of the lanthanide oxides to form carbonates (17, 18); consequently, all the samples were extensively cleaned at 973 K in a flowing mixture of 9.8% O_2 in He until no CO_2 was detected by gas chromatography. Direct NO decomposition was then measured on these oxidized REO samples between 773 and 973 K using 2.0% NO in He at a flow rate of 40 ml (STP)/min, except for La_2O_3 over which 4.0% NO at 5 ml(STP)/min was used. It was found that all the REOs tested were active for direct NO decomposition above 773 K, except for CeO_2 and Tm_2O_3, which had detectable activity only above 823 K. Because of the gas-phase reaction between O_2 and unreacted NO to form NO_2 downstream of the reactor, the O_2 and N_2 products were not in a stoichiometric ratio and, in fact, only a small amount of O_2 was observed at higher conversions. Arrhenius plots of NO decomposition rates are shown in Fig. 3, and the corresponding activation energies for this reaction are listed in Table 3. The activities for direct NO decomposition over the REOs were generally low at 773 K, but continuously increased up to 973 K, the highest temperature employed in this work. No deactivation was found over these REO catalysts during a 3-h period at 973 K. The activation energies varied from 21 to 29 kcal/mole, which are comparable to that of 22 kcal/mole for Cu/ZSM-5 (19) and 28 kcal/mole for Co_3O_4 (20). The activation energies are higher over Sr-doped La_2O_3 and Sm_2O_3 than over the pure parent oxides.

Table 3 summarizes the rates, specific activities, and TOFs for NO decomposition to N_2 at 773 K, and corresponding specific activities obtained at 973 K are presented in Fig. 4. Among the REOs tested, Sm_2O_3 was the most active catalyst for NO decomposition at both 773 and 973 K, while no detectable amount of N_2 was observed over CeO_2 and Tm_2O_3 at 773 K. On a gram basis, all the REO catalysts had activities comparable to Mn_2O_3 and MnO_2 (21), but lower than Co_3O_4 and Cu/ZSM-5 at 773 K and, in particular, the activity of Cu/ZSM-5 was 3–4 orders of magnitude higher than that of the REO catalysts (19). When specific activities for NO decomposition are compared, Sr/La_2O_3 became the most active catalyst at 973 K although Sm_2O_3 remained the most active at 773 K. The specific activities for NO decomposition over the REOs were closer to that for Mn_2O_3, although they were still lower than for Co_3O_4 (20). Cu/ZSM-5 cannot be compared on this basis because its surface area was not reported. When normalized on a TOF basis, the activities of all the REOs were even closer, particularly at 973 K, and Nd_2O_3 had the highest value (4.3×10^{-4} s^{-1}) at 773 K.

NO Reduction by CH_4 in the Absence of O_2

The reaction of NO reduction by CH_4 over these rare earth oxides was studied between 773 and 973 K using a stoichiometric NO/CH_4 ratio of 2.0% NO, 0.51% CH_4 in He at a total flow rate of 40 ml/(STP)/min (20 ml/min for La_2O_3). All the REO catalysts were active for NO reduction by CH_4 at 773 K, the activities continuously increased with temperature, and no deactivation was observed during a 3-h period at 973 K. Arrhenius plots of N_2 formation over

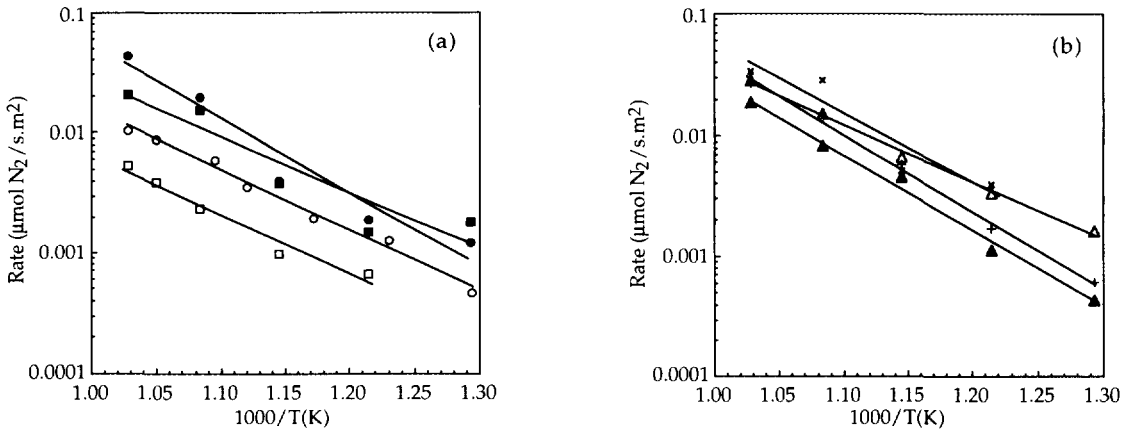

FIG. 3. Temperature dependencies of direct NO decomposition over (○) La_2O_3, (●) Sr/La_2O_3, (□) CeO_2, (■) Nd_2O_3, (△) Sm_2O_3, (▲) Sr/Sm_2O_3, (×) Tm_2O_3, and (+) Lu_2O_3.

these REOs are shown in Fig. 5, and the corresponding activation energies are presented in Table 4. N and C mass balances were within ±2.5% thus indicating that little or no NO_2 was formed although the GC column used did not separate NO_2 as a well-defined peak (14). Except for a small amount of N_2O in the product stream with a concentration that was routinely near that of the impurity N_2O level in the feed (ca. 100 ppm), nitrogen was essentially the only N-containing product detected over La_2O_3 (15), Lu_2O_3, CeO_2, Nd_2O_3, and Tm_2O_3. Therefore, the net rate of N_2O formation was near zero and the selectivities of NO conversion to N_2 were close to 100%. However, noticeable amounts of N_2O were observed over Sr/La_2O_3, Sm_2O_3, and Sr/Sm_2O_3, particularly at low temperature, and selectivity to N_2 dropped to 80–95% at lower temperatures but increased with increased temperature.

Table 4 summarizes the rates, specific activities, and TOFs at 773 K for N_2 formation during NO reduction by CH_4 in the absence of O_2 over the REOs as well as Li/MgO and Co/ZSM-5. The specific activities obtained at

TABLE 3

Direct NO Decomposition to N_2 and O_2 at 773 K, P_T = 1 atm, P_{NO} = 15.4 Torr

Catalyst	E_a (kcal/mol)	Rate of N_2 formation (μmol/s·g × 10^3)	Specific activity (μmol N_2/s·m^2 × 10^3)	TOF (s^{-1} × 10^3)	Ref.
La_2O_3	23	0.80	0.23[b]	0.60	This study
Sr/La_2O_3	28	1.4	0.83	1.4	This study
CeO_2	23	0.55[a]	0.22[a]	1.3[a]	This study
Nd_2O_3	21	3.8	1.1	4.3	This study
Sm_2O_3	22	12	1.6	3.6	This study
Sr/Sm_2O_3	29	3.0	0.44	1.5	This study
Tm_2O_3	26	1.1[a]	1.2[a]	2.0[a]	This study
Lu_2O_3	29	1.5	0.61	1.2	This study
Cu/ZSM-5	22	11600[b]	—	—	(19)
Co_3O_4	28	26[b]	3.2[b]	—	(20)
Mn_2O_3	11	4.0	0.14[b]	—	(21)
MnO_2	15	0.41	0.029[b]	—	(21)
La_2O_3	16	—	0.24[b]	—	(22)
CeO_2	18	—	0.094[b]	—	(22)
Nd_2O_3	25	—	0.14[b]	—	(22)
Sm_2O_3	14	—	0.25[b]	—	(22)
Tm_2O_3	28	—	0.030[b]	—	(22)
Lu_2O_3	26	—	0.055[b]	—	(22)

[a] Extrapolated values.
[b] Rate calculated at 773 K and P_{NO} = 15.4 Torr assuming first-order dependence.

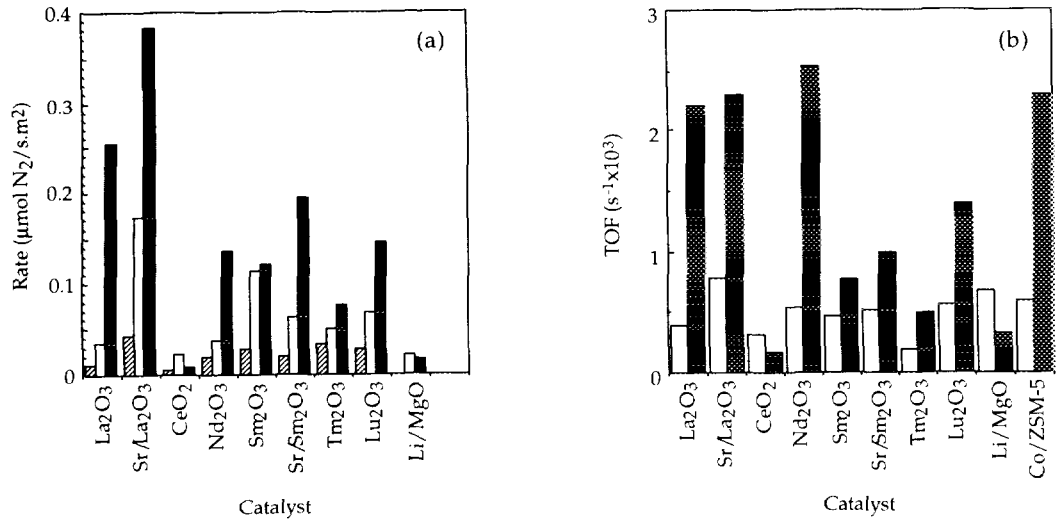

FIG. 4. (a) Specific activities at 973 K: (▨) NO decomposition, (□) NO reduction by CH_4 and, (■) NO reduction by CH_4 in the presence of 1% O_2; partial pressures as stated in Results. (b) Turnover frequencies at 773 K based on NO_{ad} at 300 K: (□) NO reduction by CH_4 and (■) NO reduction by CH_4 in the presence of 1% O_2: partial pressures as stated in Results.

973 K are presented in Fig. 4a. On a gram basis, Sr/La_2O_3 and Sr/Sm_2O_3 were the most active catalysts at both 773 and 973 K, although they were much less active than Co/ZSM-5 at 773 K. When specific activities and TOFs are compared, Sr/La_2O_3 was clearly the most active and was even more active than Co/ZSM-5, as shown by the TOFs at 773 K depicted in Fig. 4b. Li/MgO had a low specific activity, but the TOFs on all these surfaces, including Li/MgO and Co/ZSM-5, are remarkably similar, with the possible exception of Tm_2O_3. Every rate of N_2 formation via CH_4 reduction was higher than the corresponding rate for direct NO decomposition, indicating that CH_4 enhances the activity for NO conversion to N_2.

NO Reduction by CH_4 in the Presence of O_2

The effect of dioxygen on the activity and selectivity of NO reduction by CH_4 on the REOs was also investigated between 773 and 973 K using a mixture of 1.8% NO (2.0% for La_2O_3), 0.45% CH_4 (0.51% for La_2O_3), and 1.0% O_2 in He at a total flow rate of 44.5 ml(STP)/min (40 ml/min for La_2O_3). Again it was found that all the REOs were active at 773 K, the rates of N_2 formation continuously increased with temperature up to 973 K, and no bend-over behavior was observed as long as sufficient CH_4 was present in the catalyst bed. Because of NO_2 formation downstream from the reactor due to the gas-phase reaction between NO and O_2, the selectivity of NO conversion to

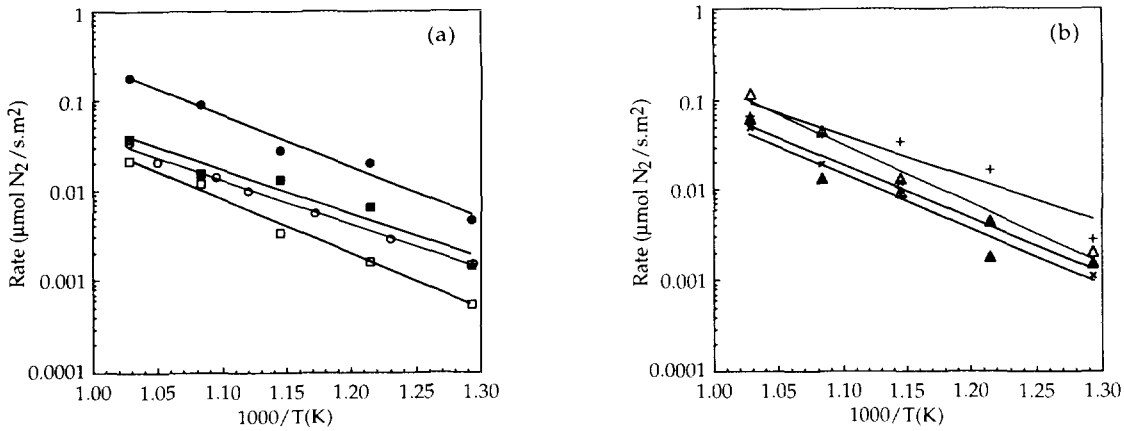

FIG. 5. Temperature dependencies of NO reduction by CH_4 in the absence of O_2 over: (○) La_2O_3, (●) Sr/La_2O_3, (□) CeO_2, (■) Nd_2O_3, (△) Sm_2O_3, (▲) Sr/Sm_2O_3, (×) Tm_2O_3, and (+) Lu_2O_3; P_{NO} = 15.4 Torr, P_{CH_4} = 3.84.

TABLE 4

NO Reduction by CH_4 at 773 K (No O_2), P_T = 1 atm, P_{NO} = 15.4 Torr, P_{CH_4} = 3.8 Torr

Catalyst	E_a (kcal/mol)	Rate of N_2 formation (μmol/s·g × 10^3)	Specific activity (μmol N_2/s·m^2 × 10^3)	TOF (s^{-1} × 10^3)
La_2O_3	24	5.3	1.5	0.39
Sr/La_2O_3	26	7.8	4.6	0.78
CeO_2	28	1.3	0.54	0.31
Nd_2O_3	22	4.9	1.4	0.54
Sm_2O_3	32	15	2.1	0.46
Sr/Sm_2O_3	28	11	1.6	0.51
Tm_2O_3	28	1.0	1.1	0.19
Lu_2O_3	22	6.8	2.8	0.56
Li/MgO	31[a]	1.8[a]	0.50[a]	0.67
Co/ZSM-5[a]	—	332[a]	1.7[a]	0.59

[a] From Ref. (14).

N_2 could not be quantitatively determined in these experiments. Figure 6 shows Arrhenius plots for the rate of N_2 formation over the various REOs, and the corresponding activation energies, presented in Table 5, varied from 22 to 29 kcal/mol and were quite similar to those in the absence of O_2.

Table 5 summarizes the rates, specific activities, and TOFs at 773 K for N_2 formation via NO reduction by CH_4 in the presence of O_2, while specific activities obtained at 973 K are presented in Fig. 4a. On a gram basis, La_2O_3 was the most active catalyst, while CeO_2 was much less active than all the other REOs and Co/ZSM-5 was again 1–2 orders of magnitude more active. However, the specific activities of all the REOs except CeO_2 were comparable to that of Co/ZSM-5 based on its apparent BET "surface area," with Sr/La_2O_3 having the highest value, which was double that of Co/ZSM-5. A comparison of TOFs, provided also in Fig. 4b, shows almost identical values on La_2O_3, Sr/La_2O_3, Nd_2O_3, and Co/ZSM-5 at 773 K. Specific activities and TOFs in this reaction were higher in the presence of O_2 than in its absence, thus indicating that O_2 facilitates NO reduction to N_2 except with the two worst catalysts—CeO_2 and Li/MgO—which had activities that were lower in the presence of O_2 (14).

In the presence of O_2, methane can react not only with nitric oxide but also with O_2 via combustion, as illustrated by reactions [1] and [2]. Total methane conversion frequently increased rapidly with temperature and the selectivity of CH_4 reacting with NO typically decreased as temperature increased before reaching a nearly constant value, as shown in Fig. 7. No higher hydrocarbons due to the

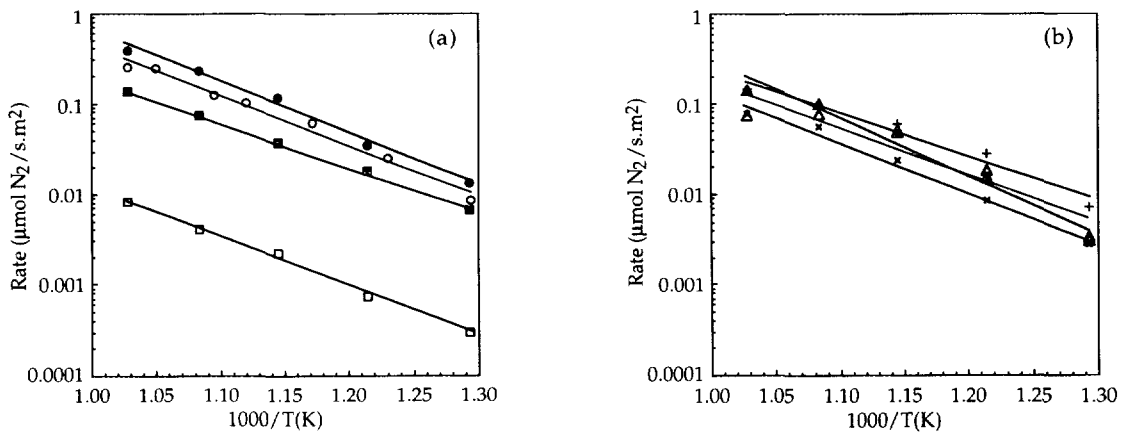

FIG. 6. Temperature dependencies of NO reduction by CH_4 in the presence of 1% O_2 over: (○) La_2O_3, (●) Sr/La_2O_3, (□) CeO_2, (■) Nd_2O_3, (△) Sm_2O_3, (▲) Sr/Sm_2O_3, (×) Tm_2O_3, and (+) Lu_2O_3; P_{NO} = 13.8 Torr, P_{CH_4} = 3.45 Torr.

TABLE 5

NO Reduction by CH_4 at 773 K in the Presence of 1% O_2, P_T = 1 atm, P_{NO} = 13.8 Torr, P_{CH_4} = 3.5 Torr

Catalyst	E_a (kcal/mol)	Rate of N_2 formation (μmol/s·g × 10^3)	Specific activity (μmol N_2/s·m^2 × 10^3)	TOF (s^{-1} × 10^3)
La_2O_3	26	30	8.5	2.2
Sr/La_2O_3	26	22	13	2.3
CeO_2	28	0.75	0.30	0.17
Nd_2O_3	22	23	6.7	2.54
Sm_2O_3	23	25	3.5	0.77
Sr/Sm_2O_3	29	21	3.2	1.0
Tm_2O_3	25	2.7	2.9	0.49
Lu_2O_3	22	18	7.3	1.4
Li/MgO	35[a]	0.84[a]	0.24[a]	0.32
Co/ZSM-5	—	1280[a]	6.6[a]	2.3

[a] From Ref. (14) and apparent BET "surface area" in Table 2.

oxidative coupling of methane were detected in the presence of oyxgen under any circumstances.

DISCUSSION

This study has confirmed that certain REOs and promoted REOs not only are quite active for the decomposition and reduction of NO_x, but also have significant surface coverages after NO chemisorption at temperatures below those used for reaction. After either calcination and evacuation at 973 K or calcination and cooling in O_2 to 300 K, substantial amounts of NO were irreversibly adsorbed on these REO surfaces at 300 K. Table 2 shows the uptakes after the former pretreatment. The presence of strongly adsorbed NO species on La_2O_3 has been further confirmed by recent TPD and XPS experiments (23). The irreversible NO uptakes varied from 4.3 to 32.8 μmol/g on these different REOs, but when they were normalized to the respective BET surface areas, the differences became smaller and all were around 2–3 × 10^{18} molecules/m^2, except for CeO_2. As expected, the irreversible NO uptake on Co/ZSM-5 was very high per gram, but the surface concentration was comparable to or lower than those on the REO samples. Li/MgO had both the lowest NO uptake and the lowest surface concentration. Assuming that one NO molecule is adsorbed per site, the results indicate that the surface coverages of adsorbed NO on these different REOs at 300 K were rather similar. It is not known at this time why the Sr doping enhanced the site density of La_2O_3 but decreased the site density for Sm_2O_3. Using these saturation coverages at 300 K as a measure of adsorption site density, TOFs for N_2 formation via both NO decomposition and NO reduction by CH_4 were obtained. Although the site density determined by irreversible NO adsorption at 300 K may not represent the *active* site density under reaction conditions, it should represent an upper limit; for example, the irreversible NO uptake over La_2O_3 at 573 K was smaller than that at room temperature.

NO adsorption and decomposition on metal oxides, including metal ion-exchanged zeolites, has been an interesting subject for some years (3, 24). Different types of adsorbed NO species have been observed, primarily by IR spectroscopy, and it has been proposed in most cases that NO adsorbs with the N atom nearest the surface although some authors have suggested that NO adsorbs with the O atom coordinated to anion vacancies at the surface (24). During NO adsorption on metal oxides it might be expected that charge transfer occurs via an electron from the oxide to the antibonding orbital of the NO molecule, thus reducing the NO bond order form 2.5 to 2.0 and making the molecule less stable than it is in the neutral state. Solids that are good electron donors should then make effective catalysts according to this scheme. However, although NO species have been observed (3), most experiments have shown electron transfer in the other direction to form NO^+ species (3, 24, 25), which have a bond order of 3.0., i.e., they should be an even more difficult entity to dissociate than the neutral NO molecule. Our present work has shown that the irreversible NO uptake on an evacuated La_2O_3 surface is higher than that on an oxidized surface, which may indicate the formation of NO^- species by electron transfer from the catalyst to NO upon adsorption. Further work is being conducted to characterize adsorbed NO species and charge transfer between NO and La_2O_3. Exposure to O_2 at 300 K prior to NO adsorption at 300 K on the evacuated La_2O_3 surface had no effect, simply because no irreversible O_2 adsorption occurred at this temperature; however, NO adsorption on La_2O_3 at 573 K resulted in a smaller uptake of 11.0 μmol/g. Our recent TPD studies of NO adsorption on La_2O_3 showed two NO

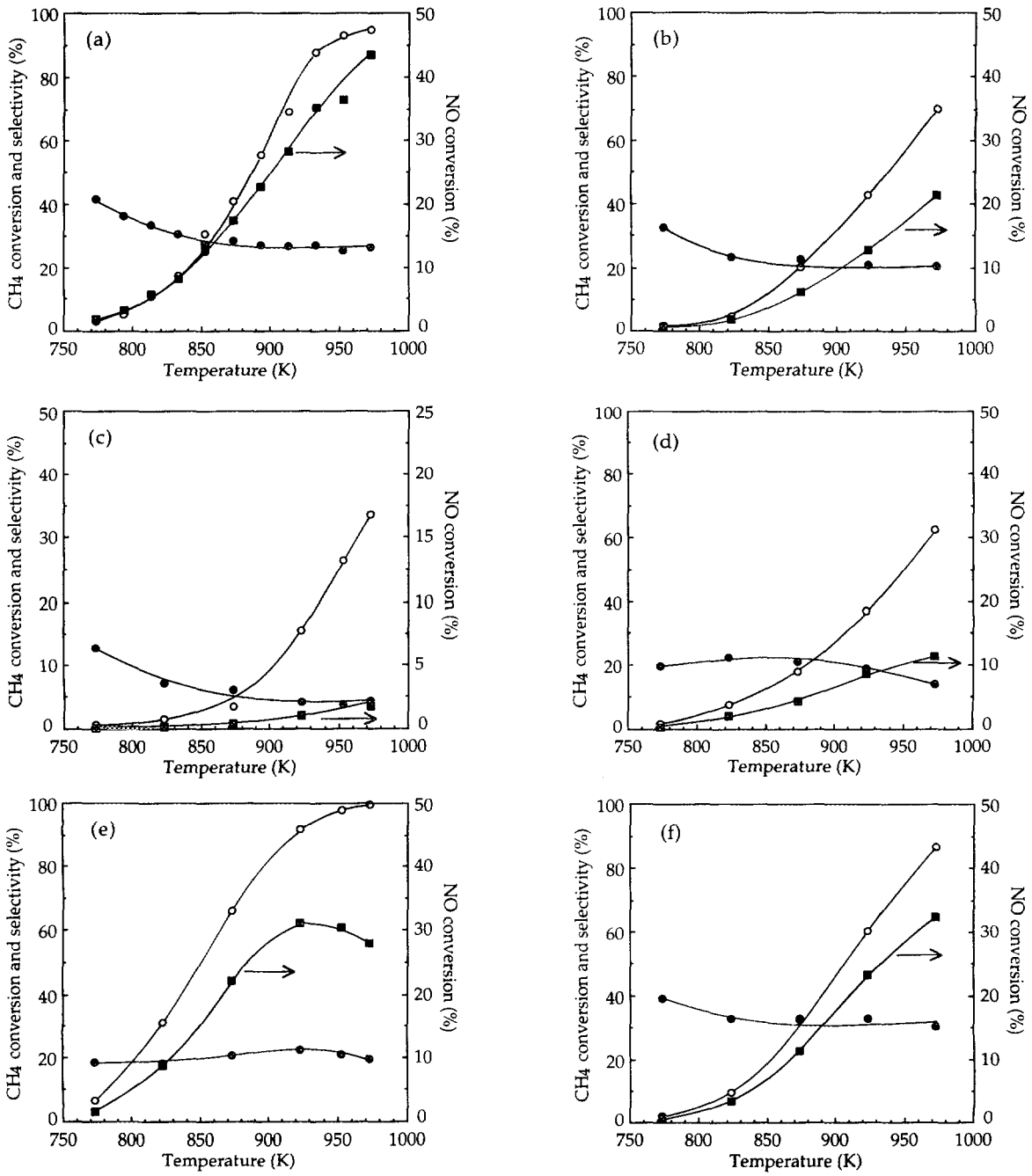

FIG. 7. NO conversion (■), CH_4 conversion (○), and selectivity for CH_4 reacting with NO (●) over: (a) La_2O_3, (b) Sr/La_2O_3, (c) CeO_2, (d) Nd_2O_3, (e) Sm_2O_3, (f) Sr/Sm_2O_3, (g) Tm_2O_3, and (h) Lu_2O_3; P_{NO} = 13.8 Torr, P_{CH_4} = 3.45 Torr, and P_{O_2} = 7.60 Torr.

desorption peaks, with the first one occurring at 473 K (23); therefore, irreversible NO adsorption at 573 K should be smaller by this amount.

Although methane activation has attracted much academic and industrial interest, studies of methane adsorption on either metal or metal oxide surfaces have not been extensive due in part to the fact that it is difficult to get methane to bond on these surfaces. Li and Xin have used FTIR to study methane adsorption and activation at 173 K on one rare earth oxide—CeO_2 (20 m^2/g), and four distinct IR bands at 3008, 2990, 2875, and 1308 cm^{-1}, due to adsorbed CH_4, were observed at 173 K (26). At elevated

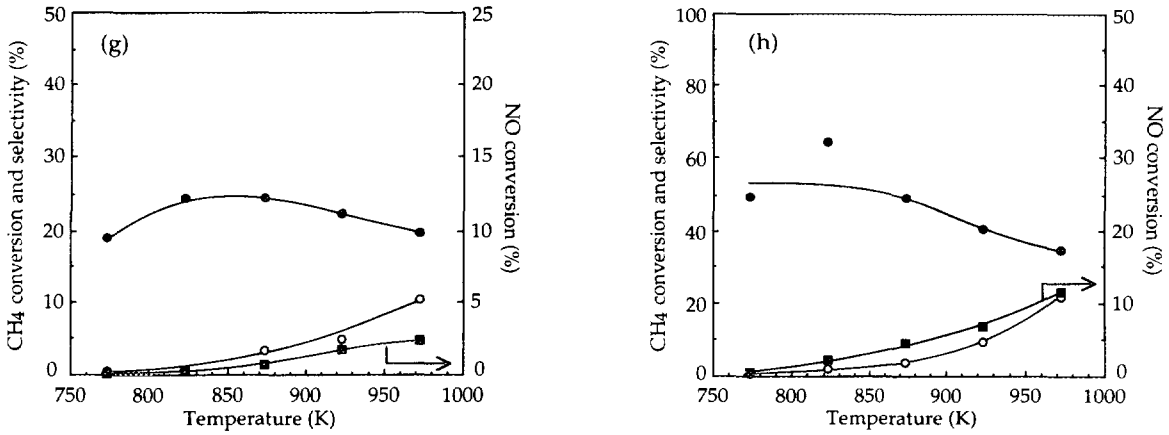

FIG. 7—*Continued*

temperatures, however, the intensities of these bands were continuously attenuated and all the bands had disappeared at 273 K, indicating that the adsorbed methane species was weakly bound; CH_4 chemisorption in the present work showed no measurable amount of strongly adsorbed CH_4 on either La_2O_3 or Sm_2O_3 at 300 or 573 K. However, it has been reported that large amounts of CH_4 were adsorbed on Sm_2O_3 between 773 and 973 K (27). When switching from CH_4 to CD_4 in an isotopic transient experiment at 973 K in the presence of 10% O_2, the amount of adsorbed methane was determined to be ~1000 μmol/g with an uncertainty of a factor of 2, and it decreased to ~330 μmol/g in the absence of O_2 (27). Without knowing all experimental details, it is hard to explain such a large amount of adsorption of a stable molecule like CH_4 on a low surface area oxide at this high temperature; for example, the assumption of a surface area of 10 m^2/g provides the coverage 6×10^{19} molecules/m^2, i.e., over a monolayer. More surprising, the amount of adsorbed CH_4 was found to be independent of temperature in the range 773–973 K. Surface carbonate groups may be the possible cause for these results.

Regarding the interaction of oxygen with REOs, information about adsorption properties and oxygen ion mobility in the solids has been gained by studying the isotopic exchange of gas-phase O_2 molecules (28). Sokolovskii *et al.* observed a pronounced influence of pretreatment conditions on isotopic exchange rates over La_2O_3 and Sm_2O_3 (29). Samples which had been preconditioned in vacuum at 973 K showed considerably higher activities for isotopic exchange at all temperatures compared to those equilibrated in oxygen prior to reaction; this effect was attributed to the formation of anion vacancies during the vacuum aging process. As described in the experimental section, all samples in the present study were pretreated at 973 K in ~10% O_2/He to remove surface carbon species and they were then evacuated at this temperature before being cooled to 300 K prior to gas admission. Even after this pretreatment, no measurable O_2 was detected at 300 K, and this absence of chemisorption was consistent with ESR studies conducted under the same conditions (30). However, when the La_2O_3 sample was exposed to O_2 at 923 K and then cooled to 110 K in O_2, an appreciable amount of adsorbed O_2^- was detected by ESR. These results show that oxygen does not chemisorb on La_2O_3 and Sm_2O_3 at 300 K, presumably because dissociative adsorption is involved and high temperatures are required to activate this process. Indeed, irreversible O_2 uptakes on La_2O_3 and Sm_2O_3 of 1.4 and 1.0 μmol/g, respectively, were observed at 573 K, which could represent oxygen atoms filling some of the vacancies created by the high-temperature annealing.

All the data presented in this paper were obtained on catalysts with stable BET surface areas. As shown in Table 1, the differences in the BET surface areas of fresh and used samples were very small and within experimental uncertainty, thus indicating that these oxides were very stable under the reaction conditions used. This stability is attributed to the fact that the highest reaction temperature in this study was 973 K, which was 50 K lower than the calcination temperature 1023 K employed for 10 h. For comparison, the activity of each REO for NO conversion to N_2 in this study is expressed in three different ways: (1) a rate, μmol $N_2/s \cdot g$; (2) a specific activity, μmol $N_2/s \cdot m^2$; and (3) a turnover frequency (TOF), molecule $N_2/s \cdot$site. Tm_2O_3 had a very low BET surface area and CeO_2 had a very low irreversible NO uptake which could have led to a high specific activity and a high TOF, respectively, although their rates are among the lowest. At high temperatures, activities over Co/ZSM-5 become much less favor-

able in comparison with REOs because they severely decrease with increasing temperature above 700–800 K in the presence of O_2.

All these low surface area REOs had detectable activity for direct NO decomposition at 773 K except for CeO_2 and Tm_2O_3, which were active only at high temperatures, and activation energies fell between 21–29 kcal/mol. Winter has studied the catalytic decomposition of NO over a number of REOs in a batch reactor system in which the rates were determined by total pressure variation after adsorption (22). This author also found that all the REOs were active, but the temperatures for NO decomposition were generally higher than those reported in the present work and the rates of NO decomposition were typically lower when compared at 773 K. Because of the method used for the rate measurement, the formation of any O_2 or gas-phase NO_x product could give rise to significant experimental errors, particularly at low temperatures, where the NO conversion was low, i.e., any variation in the assumed reaction stoichiometry $4NO(g) \rightarrow N_2(g) + 2NO_{2(ad)}$ would cause an error in apparent rate (22). Cu/ZSM-5 has been found to be much more active than all other catalysts at low temperature, but its activity severely decreases at high temperature (19).

A comparison of the rates for direct NO decomposition and those for reduction by CH_4 (see Tables 3 and 4) shows that CH_4 clearly enhances the NO conversion; for example, the activities over Sr/La_2O_3 increased by a factor of 5.5 while the respective activation energies for these two reactions remained quite similar. CeO_2, Sm_2O_3, and Lu_2O_3 showed a somewhat larger variation in E_a values. The promotional effect of CH_4 on NO conversion to N_2 might be expected on the basis that CH_4 can facilitate the removal of surface oxygen left behind by the decomposition of nitrogen oxide species. This would be particularly apparent if the rate-determining step were the removal of surface oxygen. Indeed, CO_2 was observed instead of O_2 in the presence of CH_4, indicating an interaction between CH_4 and surface oxygen. CO was not detected in these experiments; however, its peak overlaps with NO in the chromatogram so that even if some CO were formed it would be obscured by the large NO peak. Regardless, CO, once formed, could rapidly react with NO to produce N_2 and CO_2. The selectivities of NO conversion to N_2, rather than N_2O, were essentially 100% over La_2O_3, Lu_2O_3, CeO_2, Nd_2O_3, and Tm_2O_3. However Sr/La_2O_3, Sm_2O_3, and Sr/Sm_2O_3 produced noticeable amounts of N_2O under the same conditions, i.e., 5 to 20% of the product was N_2O. The N mass balance indicated that there were only small amounts, if any, of other N-containing compounds such as NO_2. As proposed previously, N_2O could be an intermediate during NO reduction by methane (15); thus the amount of N_2O in the products would depend on the relative rates of NO conversion and N_2O decomposition to N_2. Interestingly, N_2O was observed only with the most active catalysts for NO reduction. Over these catalysts the rate of N_2O decomposition may not be significantly higher than that of NO reduction, thus resulting in some undecomposed N_2O (31), while over other catalysts the rate of N_2O decomposition was presumably much higher than the rate of NO reduction, which resulted in no N_2O detected in the reaction products (15).

Perhaps of greater importance, the presence of excess O_2 promotes NO reduction by CH_4 over all the catalysts except CeO_2 and Li/MgO (see Tables 4 and 5), and the magnitude of the activity increase differed. For example, the activity on La_2O_3 at 773 K increased by a factor of about 6 in the presence of oxygen, while that on Sm_2O_3 increased less than twofold. As discussed in a previous paper (15), the role of dioxygen in NO reduction by CH_4 over the rare earth oxides is not likely due to the formation of NO_2 as an intermediate, as suggested for zeolite catalysts (32–34), rather it is presumed to promote the activation of CH_4 via the formation of methyl radicals, which are assumed to remain on the surface at these lower temperatures. Chajar *et al.* recently reported that as reduction of NO_2 by propane occurred over a Cu/MFI zeolite catalyst, a partial decomposition of NO_2 to create O_2 was responsible for an increase in activity via the partial oxidation of propane (35). It is not known why the presence of excess oxygen inhibits NO conversion to N_2 over CeO_2 and Li/MgO under the same conditions; however, CeO_2 is not a good methane oxidative coupling catalyst. Total CH_4 conversion on CeO_2 varied from ~1% at 773 K to ~35% at 973 K, which was much lower than CH_4 conversions over other REOs; therefore, the activity decrease in the presence of O_2 is not due to a much lower CH_4 concentration caused by combustion. It is perhaps surprising that CeO_2 has the lowest activity for both direct NO decomposition and reduction by CH_4 in the absence of oxygen as CeO_2 has been widely used as a promoter in three-way automotive exhaust catalysts (36).

Correlations between catalytic activity and properties of the rare earth oxides have always been interesting subjects because of gradual changes caused by the lanthanide contraction. Takasu *et al.* found similarities between activity for NO oxidation to NO_2 and that for isotopic oxygen exchange, suggesting that the rate-determining processes of each reaction were closely related (37). In a study of CO hydrogenation over REO-supported Pd, Vannice *et al.* found that the CH_4 turnover frequency decreased as the activation energy for electrical conductivity increased in the REO support, whereas the CH_3OH turnover frequency was dependent on the atomic number of the REOs and decreased with the lanthanide contraction (38). In the present work no correlation could be found between any catalytic activity and a given property of the REOs, such as electron configuration, covalent and ionic radii, or acti-

vation energy for electron conductivity. However, we have found that good methane oxidative coupling catalysts are also active NO reduction catalysts; for example, La_2O_3 and Sm_2O_3 are two of the best catalyst systems reported for methane oxidative coupling (39–41). Doping La_2O_3 with strontium improves both activity and selectivity for oxidative coupling (40), and our study has shown it also provides a significant increase in specific activity for NO reduction by CH_4. Nd_2O_3 is a moderately active catalyst for oxidative coupling (42, 43), while CeO_2 is completely nonselective for C_2 hydrocarbon formation, although it is active for total oxidation to CO_2 (41). All these observations are consistent with the present results for NO reduction by CH_4 over these REOs and support our belief that these two reactions are closely related in terms of methane activation, presumably involving methyl radicals (14). The precise mechanism is not known at this time; however, both surface O atoms (44) and surface vacancies, i.e., F centers (45), have been proposed to activate CH_4 via $CH_3\cdot$ radicals.

It is important to compare these REO catalysts with other catalysts which can also reduce NO to N_2 by CH_4. After studying a number of zeolite catalysts, Li and Armor found that Co/ZSM-5, Ga/H-ZSM-5, and Ga/H-mordenite were particularly active for NO reduction by CH_4 in the presence of O_2 (5–8). When the reaction was conducted at 773 K in a gas mixture of 1610 ppm NO, 1000 ppm CH_4, and 2.5% O_2 at a GHSV of 30,000 h^{-1}, the rates of N_2 formation over Co/ZSM-5 and Ga/ZSM-5 were 0.18 and 0.20 μmol/s · g, respectively (8), which are about 1–2 orders of magnitude higher than those of the REO catalysts at the same temperature after correction for the NO pressure dependence. The rate of N_2 formation over Co/ZSM-5 is enhanced at higher NO concentrations (15). When compared in terms of either specific activity or TOF, the REOs are comparable to Co/ZSM-5 for NO reduction by CH_4 in the presence of O_2, as shown in Table 5. Furthermore, the activity of each REO continuously increased with reaction temperature, except for Sm_2O_3, and the activities at 973 K are about 20–30 times higher than those at 773 K, whereas both Co/ZSM-5 and Ga/H-ZSM-5 showed a decrease in activity above 773 K, particularly for Co/ZSM-5 (8). It is clear from Fig. 7e that the decrease in NO conversion does not happen until almost all the CH_4 is combusted, behavior which can be attributed to CH_4 depletion, as previously proposed for zeolite catalysts (5). Figure 8 verifies this behavior for Co/ZSM-5 at higher NO and CH_4 pressures. Nevertheless, as long as sufficient CH_4 is present, oxygen promotes NO reduction to N_2 by CH_4 on both the zeolite and REO catalysts (except for CeO_2) which may indicate similar chemistry associated with the formation of reaction intermediates involving oxygen.

Before comparing the selectivity of methane reactions over different catalysts, it is worthwhile to discuss the definition of selectivity. Without knowing further details about

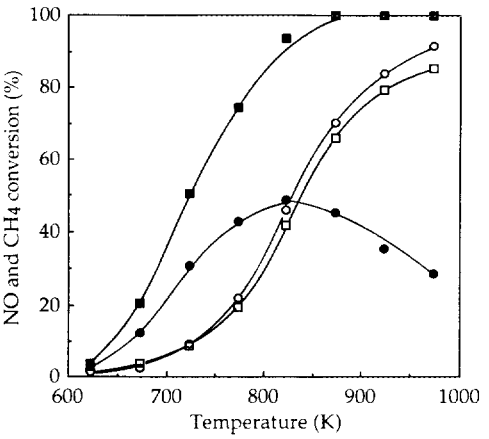

FIG. 8. NO conversion over 4% Co/ZSM-5 (0.1 g) vs temperature using 1.8% NO, 0.45% CH_4 in He in the absence of O_2 (○, NO; □, CH_4) and in the presence of 1% O_2 (●, NO; ■, CH_4), at a total flow rate of 44.5 ml(STP)/min.

the manner in which oxygen participates during NO reduction by CH_4, it is difficult to be precise about the manner by which methane reduces NO to N_2. In the present work, the definition of methane selectivity given by reaction [3] is based on the competitive oxidation of CH_4 by either NO or O_2 (reactions [1] and [2]), as suggested by Witzel *et al.* (46). Li and Armor have defined a different selectivity, α, based on reaction [2] plus the reaction

$$2NO + CH_4 + O_2 \rightarrow N_2 + CO_2 + 2H_2O \qquad [4]$$

as

$$\alpha = \frac{0.5 \times [NO]_0 \times C_{NO}}{[CH_4]_0 \times C_{CH_4}} \times 100\%, \qquad [5]$$

where $[NO]_0$ and $[CH_4]_0$ are the inlet concentrations of NO and CH_4, and C_{NO} and C_{CH_4} are the conversions of NO and CH_4 (8). Reaction [4] is actually a combination of reactions [1] and [2] obtained by assuming a ratio of 1 : 1, which means that reaction [4] is a combination of the reduction and deep oxidation reactions. This definition gives an α value higher than the selectivity defined in the present work by a factor of 2. Selectivities (S) of methane (Eq. [3]) reacting with NO to produce N_2 were about 20–40% over all the REOs, except for CeO_2 for which it was only about 5–10%. Generally, the selectivities were high at low temperatures and decreased with temperature before reaching a nearly constant value at higher temperatures, as indicated in Figs. 7a–7h. At 823 K, the selectivities of methane reacting with NO over La_2O_3, Sr/La_2O_3, Sm_2O_3, and Sr/Sm_2O_3 were 32, 23, 18, and 33% respectively, which are equivalent to the respective α values of 63, 46, 36, and

66%. These α values compare favorably with those for Co/ZSM-5 and Ga/ZSM-5, which were 22 and 82%, respectively, at the same temperature (8).

SUMMARY

This study has shown that both NO decomposition and NO reduction by CH_4 can occur readily on both pure REOs and Sr-promoted REO surfaces. Furthermore, the rate of NO reduction by CH_4 was enhanced two- to six-fold by the presence of O_2 over all the REOs examined, except CeO_2. NO chemisorption at 300 K was significant on all these surfaces and provided the highest coverage on Tm_2O_3 and Sr/La_2O_3—3.5×10^{18} molecules NO/m^2. The relative specific activities (μmol $N_2/s \cdot m^2$) for NO decomposition at 773 K were $Sm_2O_3 > Tm_2O_3$, $Nd_2O_3 > Sr/La_2O_3 > Lu_2O_3 > Sr/Sm_2O_3 > La_2O_3$, CeO_2. It is not clear yet why promotion by Sr enhances the activity over La_2O_3 but decreases it over Sm_2O_3. In the absence of O_2, the relative specific activities for NO reduction by CH_4 are $Sr/La_2O_3 > Lu_2O_3 > Sm_2O_3 > Sr/Sm_2O_3$, La_2O_3, $Nd_2O_3 > Tm_2O_3 > CeO_2$; however, the TOF values are all rather similar, except possibly for Tm_2O_3. In the presence of 1% O_2, a much wider variation (over 40-fold) in specific activity occurred for NO reduction by CH_4 and the relative order at 773 K was $Sr/La_2O_3 > La_2O_3 > Lu_2O_3 > Nd_2O_3 > Sm_2O_3 > Sr/Sm_2O_3 > Tm_2O_3 > CeO_2$. The addition of O_2 had little effect on the apparent activation energy except with Sm_2O_3. The surface chemistry associated with these catalytic processes is not yet understood and studies are under way in our laboratory to gain additional insight; however, the positive influence of both promoters and O_2 coupled with the capability to determine both specific activities and TOFs provides optimism that further improvements are possible. The role of lattice oxygen as well as the adsorbed NO_x and CH_4 species present are of particular interest in this reaction.

ACKNOWLEDGMENTS

This work was supported by the National Science Foundation under Grant CTS-9211552. We thank Dr. Y. Li and Dr. J. Armor for providing samples of metal/ZSM-5 catalysts.

REFERENCES

1. Truex, T. J., Searles, R. A., and Sun, D. C., *Plantinum Met. Rev.* **36,** 2 (1992).
2. Armor, J. N., *Appl. Catal.* **B1,** 221 (1992).
3. Iwamoto, M., *in* "Studies in Surface Science and Catalysis: Future Opportunities in Catalytic Separation Technology" (M. Misono, Y. Moro-oka, and S. Kuimura, Eds.), p. 121. Elsevier, Amsterdam, 1990.
4. Li, Y., and Hall, W. K., *J. Catal.* **129,** 202 (1991).
5. Li, Y., and Armor, J. N., *Appl. Catal.* **B2,** 239 (1993).
6. Li, Y., and Armor, J. N., *Appl. Catal.* **B1,** L31 (1992).
7. Li, Y., and Armor, J. N., *Appl. Catal.* **B3,** L1 (1993).
8. Li, Y., and Armor, J. N., *J. Catal.* **145,** 1 (1994).
9. Witzel, F., Sill, G. A., and Hall, W. K., *J. Catal.* **149,** 229 (1994).
10. Burch, R., and Millington, P. J., *Appl. Catal.* **B2,** 101 (1993).
11. Sato, S., Yu-u, Y., Yahiro, H., Mizuno, N., and Iwamoto, M., *Appl. Catal.* **70,** L1 (1991).
12. Hamada, H., Kintaichi, Y., Yoshinari, T., Tabata, M., Sasaki, M., and Ito, T., *Catal. Today* **17,** 111 (1993).
13. Burch, R., and Scire, S., *Appl. Catal.* **B3,** 295 (1994).
14. Zhang, Z., Walters, A. B., and Vannice, M. A., *J. Catal.* **146,** 568 (1994).
15. Zhang, X., Walters, A. B., and Vannice, M. A., *Appl. Catal.* **B4,** 237 (1994).
16. Xu, M. and Lunsford, J. H., *Catal. Lett.* **11,** 295 (1991).
17. Rosynek, M. P., and Magnuson, D. T., *J. Catal.* **46,** 402 (1977).
18. Sudhakar, C., and Vannice, M., *Appl. Catal.* **14,** 47 (1985).
19. Li, Y., and Hall, W. K., *J. Phys. Chem.* **94,** 6145 (1990).
20. Shelef, M., Otto, K., and Gandhi, H., *Atmos. Environ.* **3,** 107 (1969).
21. Yamashita, T., and Vannice, M. A., in preparation.
22. Winter, E. R. S., *J. Catal.* **22,** 158 (1971).
23. Zhang, X., Liu, Z.-M., and Vannice, M. A., unpublished results.
24. Hightower, J. W., and van Leirsburg, D. A., *in* "The Catalytic Chemistry of Nitric Oxides" (R. L. Klimisch and J. G. Larson, Eds.), Plenum, New York, 1975.
25. Gandhi, H. S., and Shelef, M., *J. Catal.* **28,** 1 (1973).
26. Li, C., and Xin, Q., *J. Phys. Chem.* **96,** 7714 (1992).
27. Ekstrom, A., and Lapszewicz, J. A., *J. Phys. Chem.* **93,** 5230 (1989).
28. Netzer, F. P., and Bertel, E., *in* "Handbook on the Physics and Chemistry of Rare Earths" (K. A. Gschneidner, Jr. and L. Eyring, Eds.), 1982.
29. Sokolovskii, V. D., Sazonov, L. A., Boreskov, G. K., and Moskvina, Z. V., *Kinet. Catal.* **9,** 130 (1968).
30. Liu, C. C., Zhang, X., Walters, A. B., and Vannice, M. A., in preparation.
31. Zhang, X., Walters, A. B., and Vannice, M. A., unpublished results.
32. Ansell, G. P., Diwell, A. F., Golunski, S. E., Hayes, J. W., Rajaram, R. R., Truez, T. J., and Walker, A. P., *Appl. Catal.* **B2,** 81 (1993).
33. Valyon, J., and Hall, W. K., *J. Phys. Chem.* **97,** 1204 (1993).
34. Hall, W. K., and Valyon, J., *Catal. Lett.* **15,** 311 (1992).
35. Chajar, Z., Primet, M., Praliaud, H., Chevrier, M., Gauthier, C., and Mathis, F., *Catal. Lett.* **28,** 33 (1994).
36. Harris, B., Diwell, A. F., and Hallet, C., *Platinum Met. Rev.* **32,** 73 (1988).
37. Takasu, T., Nishibe, S., and Matsuda, Y., *J. Catal.* **49,** 236 (1977).
38. Vannice, M. A., Sudhakar, C., and Freeman, M., *J. Catal.* **108,** 97 (1987).
39. Deboy, J. M., and Hicks, R. F., *J. Chem. Soc. Chem. Commun.*, 982 (1988).
40. Deboy, J. M., and Hicks, R. F., *J. Catal.* **113,** 517 (1988).
41. Sugiyama, S., Matsumura, Y., and Moffat, J. B., *J. Catal.* **139,** 338 (1993).
42. Otsuka, K., Jinno, K., and Morikawa, A., *Chem. Lett.*, 499 (1985).
43. Otsuka, K. and Nakajima, T., *Inorg. Chim. Acta.* **120,** L27 (1989).
44. Ito, T., Wang, J.-X., Lin, C. H., and Lunsford, J. H., *J. Am. Chem. Soc.* **107,** 5062 (1985).
45. Wu, M. C., Truong, C. M., Coulter, K., and Goodman, D. W., *J. Catal.* **140,** 344 (1993).
46. Witzel, F., Sill, G. A., and Hall, W. K., *J. Catal.* **149,** 229 (1994).